International Journal of Steel Structures 17(1): 19-30 (2017)
DOI 10.1007/s13296-016-0102-z
ISSN 1598-2351 (Print)
ISSN 2093-6311 (Online)

International Journal of
STEEL
STRUCTURES
www.springer.com/journal/13296

Isotropic-Kinematic Cyclic Hardening Characteristics of Plate Steels

Ashkan Shakeri*

Master student of Earthquake Engineering and Engineering Seismology (MEEES)
Department of Civil Engineering, K1 Building, Middle East Technical University, Inonu Bulvari, 06531 Ankara, Turkey

Abstract

Cyclic hardening of metals is considered as one of the most important features that affects extremely the hysteresis behavior of steel structures. One approach to study this characteristic is dividing it into two components, including isotropic hardening and kinematic hardening, and defining any of these components for any type of metals by calibrated data obtained from experiments. However, the lack of these calibrated data on metals, restricts this approach. Therefore, in this paper the isotropic and kinematic characteristics of five different steel grades from 100 to 485 MPa, under various strain ranges between ±1 and ±7% were proposed. Afterwards, four of these five grades were validated in order to find the appropriate combination of data for any of them, and to compare the result of this approach with those obtained from a well-known hardening model, Ramberg-Osgood. The results showed the high accuracy of the isotropic-kinematic hardening model in comparison to the Ramberg-Osgood method.

Keywords: high performance steel, low yield point steel, cyclic hardening, isotropic hardening, kinematic hardening

1. Introduction

An appropriate prediction of stress-strain response of structural members is a fundamental stage in modeling of their behavior (e.g. buckling behavior or cumulative damage). However, in most cases, the cyclic behavior of steel structures is not as simple as their behavior under monotonic loading, because the repetition of loads usually leads to an increase in hardening amount of these structures (Dusicka *et al*., 2004; Shi *et al*., 2011). Therefore, an exact method for estimating this over strength seems necessary, although many successful researches have been conducted studying the over strength of Seismic Force Resisting Systems (SFRSs) considering the varieties in the geometry of these systems rather than the cyclic hardening of steel materials (e.g. (Kuşyılmaz & Topkaya, 2013)).

Among many different suggested methods, the model proposed by Ramberg and Osgood (Ramberg & Osgood, 1943), which requires only three parameters, is commonly used by many researchers for predicting the cyclic hardening of steel members (e.g. (Dusicka *et al*., 2004)). Since, these parameters should be calibrated for any concerned material, experimental studies are required in this method as in any similar method. Hence, some experiments have been carried out for some metals, such as the research carried out by Dusicka *et al*. (2007).

Although Ramberg-Osgood material model gives a satisfactory hardening estimation compared with elastic-plastic material model, it was proved inexact, especially in the case of Low Yield Point (LYP) steel grades (Dusicka *et al*., 2004). Therefore, in recent years, some fundamental experimental and analytical studies have been conducted in order to improve the accuracy of cyclic hardening prediction for conventional steel as well as high yield point steel grades (e.g. (Shi *et al*., 2011; Shi *et al*., 2012; Wang *et al*., 2015)

On the other hand, the combined isotropic- kinematic hardening method (Chaboche, 1989; Lemaitre & Chaboche, 1990) is another way of simulating the cyclic hardening behavior of metals. In this solution, cyclic hardening is separated into two different components named “Isotropic” and “Kinematic”. One of the virtues of this method is that the data reflecting both or only one of the components can be directly given to ABAQUS in either forms of tabular or calibrated parameters (HKS, Hibbitt *et al*., 2012). However, lack of the required data for many of steel grades is a problem in using this method. Therefore, this paper is concentrated on isotropic and kinematic

Received March 13, 2016; accepted June 20, 2016;
published online March 31, 2017

*Corresponding author
Tel: +98 9112364700, Fax: +90 539 847 2637
E-mail: a.shakeri@meees.org, ashkan.shakeri@gmail.com

cyclic hardening characteristics of five steel grades including: Low Yield Point steel grades 100 and 225 (LYP100 and LYP225), A709-conventional grade 345 (GR345), A709-High Performance Steel (HPS) grade 485 (HPS485) and Nippon Steel BT-HT440 (HT440). First, for each of the hardening components, the required data is extracted for any of the steel grades from the experiments conducted by Dusicka *et al*. (2007) in the form of stress-strain points (curve) for any strain range between ±1 and ±7%, and then for simplicity's sake, the calibrated parameters are proposed by the use of curve regression. In the second part, in order to validate these parameters and to show the exactness of this approach, four of the links investigated (experimentally) by Dusicka *et al*. (2010) are simulated in ABAQUS to find the optimum combination of parameters from different strain ranges for four types of the steel grades. Another formulation of Ramberg-Osgood model (Ramberg & Osgood, 1943) that can be introduced directly to ABAQUS (HKS, Hibbitt *et al*., 2012) is also studied in this part.

2. Hardening Characteristics

Both of the Isotropic and Kinematic components of the combined isotropic-kinematic hardening model are discussed separately in the following:

2.1. Isotropic hardening

Isotropic hardening component indicates the evolution of the equivalent stress, which specifies the size of yield surface (σ^0), as a function of the equivalent plastic strain ($\bar{\varepsilon}^{pl}$), and can be inserted in ABAQUS as a tabular data. These data can be simply obtained for any strain range, ε ($\varepsilon_{t,\max}-\varepsilon_{t,\min}$), from a strain-controlled experiment with symmetric cycles ($\Delta\varepsilon=2\varepsilon_{t,\max}$). The plastic strain range, shown in Fig. 1, is approximately calculated by Eq. (1) (HKS, Hibbitt *et al*., 2012):

$$\Delta\varepsilon^{pl} \approx \Delta\varepsilon - 2\frac{\sigma_1^t}{E} \tag{1}$$

where σ_1^t and E are the ultimate tensile stress of the first cycle and the Young's modulus of the material.

The equivalent stress which describes the size of the yield surface is equal to σ_0 at zero equivalent plastic strain, and the peak tensile stress points are calculated for each cycle, i, by removing the kinematic component from the yield stress (HKS, Hibbitt *et al*., 2012):

$$\sigma_i^0 = \sigma_i^t - \alpha_i \tag{2}$$

where α_i is the value of backstress and can be obtained as following (HKS, Hibbitt *et al*., 2012):

$$\alpha_i = \frac{\sigma_i^t + \sigma_i^c}{2} \approx \frac{\sigma_1^t + \sigma_1^c}{2} \tag{3}$$

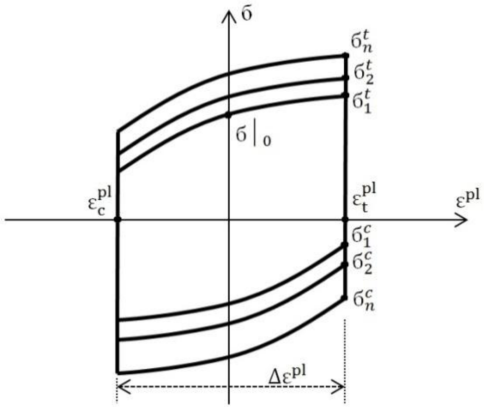

Figure 1. Cyclic strain-controlled experiment.

where σ_i^t and σ_i^c are the ultimate tensile and compressive stress values of any cycle (i), respectively. It is important to notice that as the value of back stress at a particular strain level is approximately the same for each cycle, it can be easily calculated once for one cycle (such as the first cycle as shown in the right side of Eq. (3)) and the obtained value can be utilized for every cycle. The equivalent plastic strain which corresponds to any σ_i^0 is calculated by Eq. (4):

$$\bar{\varepsilon}_i^{pl} = \frac{1}{2}(4i-3)\Delta\varepsilon^{pl} \tag{4}$$

The obtained data pairs (σ_i^0, $\bar{\varepsilon}_i^{pl}$) including the first point (σ_0, 0) can be given directly to ABAQUS in the tabulated form.

It should be noticed that these tabular values describe the size of yield surface and must be introduced for a strain range, $\Delta\varepsilon$, that matches the anticipated strain range of the analysis, as the material model estimates only the specified isotropic behavior even at other applied strain ranges during the loading. Therefore, for each part of any structure that may experience a different strain range, a specific data is required, and for the case of stepwise increasing strain-controlled loading, such as those introduced by AISC (2005) or ATC (1992), the utilization of 'field variables' (changing material properties during the nonlinear analysis) can also be helpful in achieving a higher accuracy. This technic is utilized in sections 3.2 and 3.3.

As mentioned earlier, in this paper, the isotropic characteristic of the five steel grades, naming LYP100, LYP225, GR345, HT440 and HPS485, is obtained for each strain range, from ±1 to ±7%. For this purpose, the experiments conducted by Dusicka *et al*. (Dusicka, *et al*., 2007) are utilized and Table 1 shows the monotonic mechanical characteristics of the steel types used in that experiment.

The isotropic characteristics can be easily obtained by using the Eqs. (1) to (4). As an example, the calculation trend of the data pairs corresponding to LYP225 at the strain range ±4% is briefly explained. The yield stress is

Table 1. Mechanical characteristics of the steel grades (Dusicka *et al*., 2007)

	LYP100	LYP225	GR345	HPS485	HT440
f_y (MPa)	100	225	345	485	440
E (MPa)	153100	195100	186200	201300	208200
f_{ya} (MPa)	76.5	242	353	503	501
f_{ua} (MPa)	257	324	534	590	688

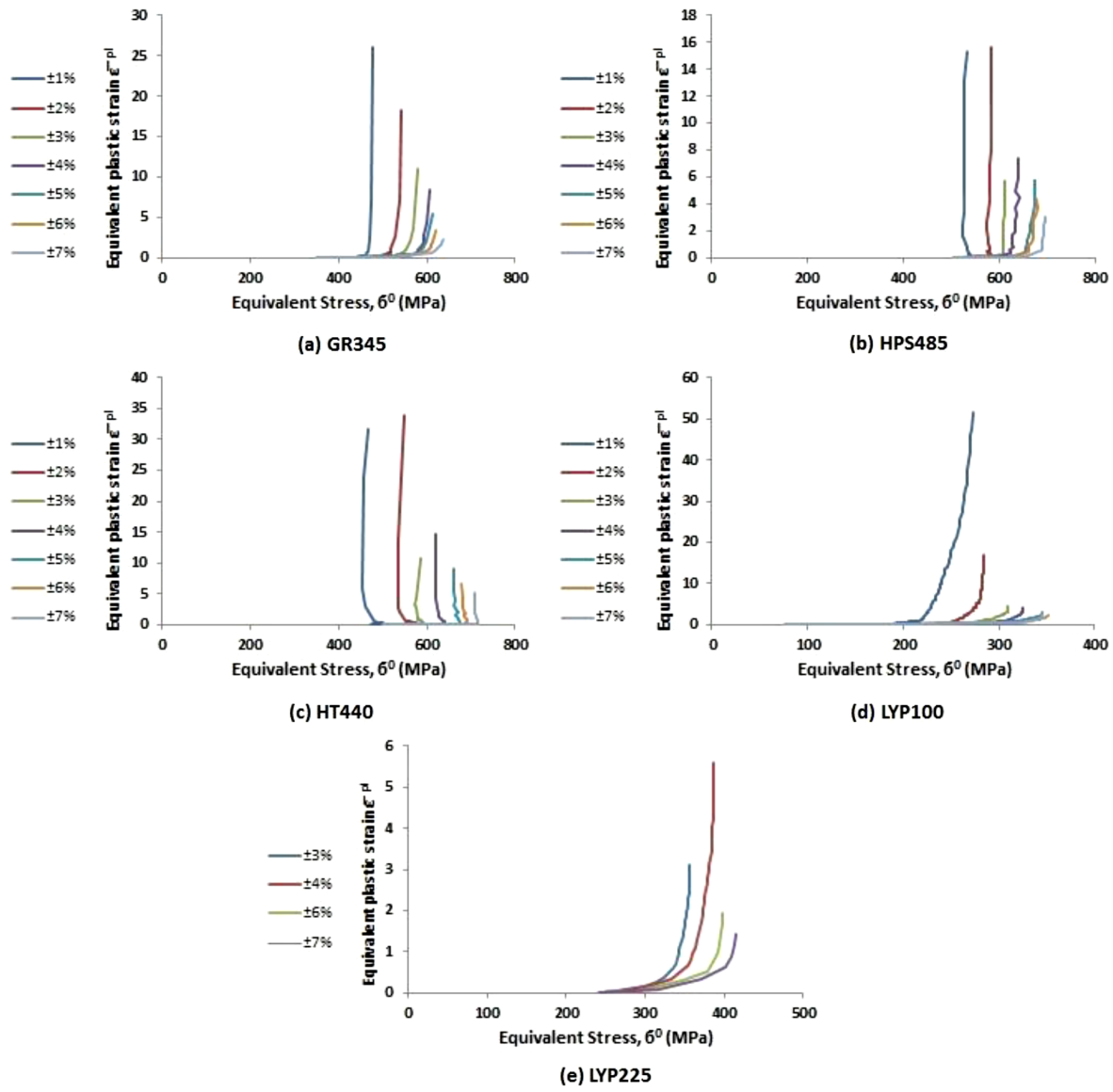

Figure 2. Isotropic characteristics.

obtained from Table 1 (242 MPa), so the point ($\sigma|_0$, 0) is equal to (242, 0). The strain range ($\Delta\varepsilon$) is calculated as ($\varepsilon_{t,\max}-\varepsilon_{t,\min}$=0.04−(−0.04)=0.08); σ_1^I and E are obtained from experimental results (Dusicka *et al*., 2007) and Table 1, respectively; and therefore, by the use of Eq. (4) plastic strain range, $\Delta\varepsilon^{pl}$, is obtained, and based on which the equivalent plastic strain at the first cycle, $\bar{\varepsilon}_1^{pl}$ can be easily obtained as $\frac{\Delta\varepsilon^{pl}}{2}$. On the other hand, utilizing Eq. (3) and the data obtained by Dusicka *et al*. (2007), α_i value is obtained; afterwards, by substituting this value in Eq. (2), σ_1^0 is calculated. As a result, the point (σ_1^0 , $\bar{\varepsilon}_1^{pl}$) is equal to (266.4, 0.039), and similarly the other points are calculated. The data pairs, for all the steel grades at every strain range are summarized as stress-strain curves in Fig. 2. It is observed that for LYP225 grade, the curves corresponding to strain ranges ±1, ±2, ±5% are not

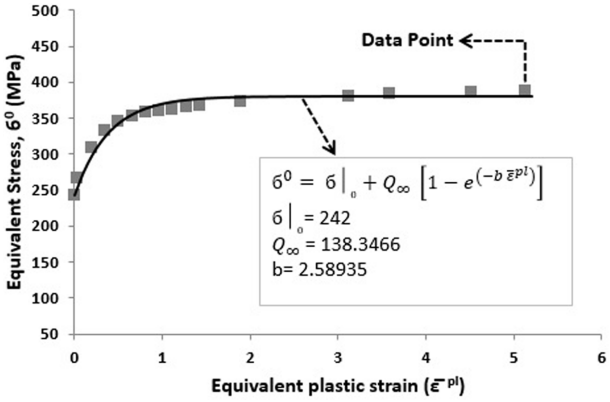

Figure 3. Regression of isotropic data for LYP225 at strain range of ±4%.

presented, and that is because of the problems occurred in the experiments of these cases which resulted in test terminations in these strain ranges (Dusicka *et al*., 2007). Also, it can be seen that in contrast to the other steel grades, HT440, not only experienced no considerable isotropic hardening, but also showed an obvious softening through the cycles.

There is also a simpler way of introducing isotropic characteristics to ABAQUS in which instead of utilizing the stress-strain curve, the isotropic hardening component is specified only by three parameters utilizing the exponential law described in Eq. (5) (HKS, Hibbitt *et al*., 2012):

$$\sigma^0 = \sigma|_0 + Q_\infty[1 - e^{(-b\bar{\varepsilon}^{pl})}] \tag{5}$$

where Q_∞ and b define the maximum changing in the size of yield surface and the rate of evolution in the size of yield surface, respectively. As an example of the curve regression for obtaining the material parameters, Q_∞ and b, for LYP225 at the strain range of ±4% is shown in Fig. 3. It is important to notice that the yield stress at zero plastic strain ($\sigma|_0$) is considered constant in either of utilizing tabulated data or parameters.

In the same way, the isotropic hardening parameters, $\sigma|_0$, Q_∞, and b, for all the cases are summarized in Table 2.

2.2. Kinematic hardening

The nonlinear kinematic component of the material model defines the displacement of the yield surface in stress area via back stress (HKS, Hibbitt *et al*., 2012). The kinematic hardening component in ABAQUS is calculated as a combination of a "*purely kinematic term*" (using "*linear Zeigler hardening law*") and a "*relaxation term*" which describes the nonlinearity (HKS, Hibbitt *et al*., 2012). There are three ways to introduce the kinematic hardening component to ABAQUS. One approach is to utilize the stress-strain data of the stabilized cycle. In this way, the cyclic loading should be repeated until the steady-state condition is obtained, in which the shape of the stress-strain curve does not evolve between two consecutive cycles. Figure 4 illustrates the required data pairs (σ_i, ε_i^{pl}). In this case, the strain axis should be defined such that the plastic strain value of the first pair is equal to zero (ε_i^{pl}=0). For this purpose, Eq. (6) shifts the strain values (ε_i) to achieve the plastic strain values (ε_i^{pl} (HKS, Hibbitt *et al*., 2012):

$$\varepsilon_i^{pl} = \varepsilon_i - \frac{\sigma_i}{E} - \varepsilon_p^0 \tag{6}$$

where ε_p^0 is described in Fig. 4.

The data pairs (σ_i, ε_i^{pl}) defining the kinematic hardening component of the material model for all the steel grades are summarized as stress-strain curves in Fig. 5.

Table 2. Isotropic parameters

Steel grade	Parameter	±1%	±2%	±3%	±4%	±5%	±6%	±7%
GR345	R0	353	353	353	353	353	353	353
	Q	114.3345	168.8759	202.0422	231.4678	236.2736	251.1475	268.3742
	b	13.26175	8.216033	8.405291	10.58755	8.518524	12.75794	12.11833
HPS485	R0	503	503	503	503	503	503	503
	Q	28.3169	75.29425	104.2219	126.8502	158.6379	164.5877	186.5062
	b	46.68021	15.01913	15.79866	13.96455	23.78051	19.62406	23.05296
HT440	R0	503	503	503	503	503	503	503
	Q	28.3169	75.29425	104.2219	126.8502	158.6379	164.5877	186.5062
	b	46.68021	15.01913	15.79866	13.96455	23.78051	19.62406	23.05296
LYP100	R0	76.5	76.5	76.5	76.5	76.5	76.5	76.5
	Q	149.3448	196.5126	224.7476	241.7943	259.5339	263.5871	261.3753
	b	6.008153	6.158717	4.876861	5.55059	5.421614	6.768276	6.582169
LYP225	R0	-	-	242	242	-	242	242
	Q	-	-	109.4573	138.3466	-	153.2311	165.9965
	b	-	-	3.70427	2.58935	-	4.320803	6.282858

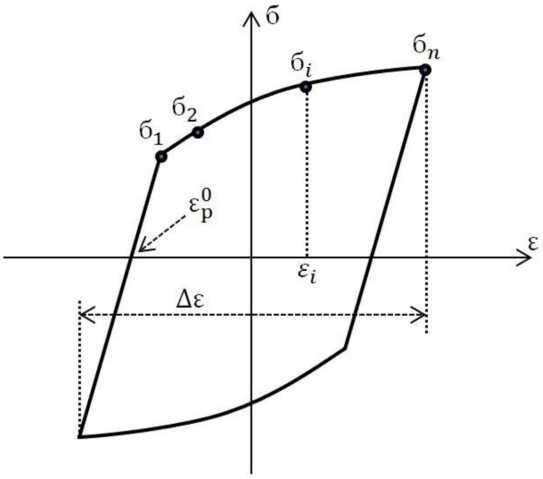

Figure 4. Kinematic data pairs.

Similar to the concept of isotropic cyclic hardening component, there is also an easier way of introducing kinematic characteristic to ABAQUS by specifying kinematic hardening parameters. Corresponding to each data pair (σ_i , ε_i^{pl}), the value of α_i (the overall backstress at the data point i), can be achieved by the use of Eq. (7) (HKS, Hibbitt *et al*., 2012):

$$\alpha_i = \sigma_i - \sigma^s \tag{7}$$

where σ^s denotes the "*Stabilized size of the yield surface*" and is calculated by Eq. (8) (HKS, Hibbitt *et al*., 2012):

$$\sigma^s = \frac{\sigma_1 + \sigma_n}{2} \tag{8}$$

The relationship of the k^{th} backstress value (α_k) and the k^{th} kinematic hardening parameters, C_k and γ_k, at any point, i, is described by Eq. (9) (HKS, Hibbitt, *et al*., 2012):

$$\alpha_k = \frac{c_k}{\gamma_k}\left(1 - e^{-\gamma_k \varepsilon^{pl}}\right) + \alpha_{k,1} e^{-\gamma_k \varepsilon^{pl}} \tag{9}$$

where $\alpha_{k,1}$ is the k^{th} backstress at the first point (σ_1 ,

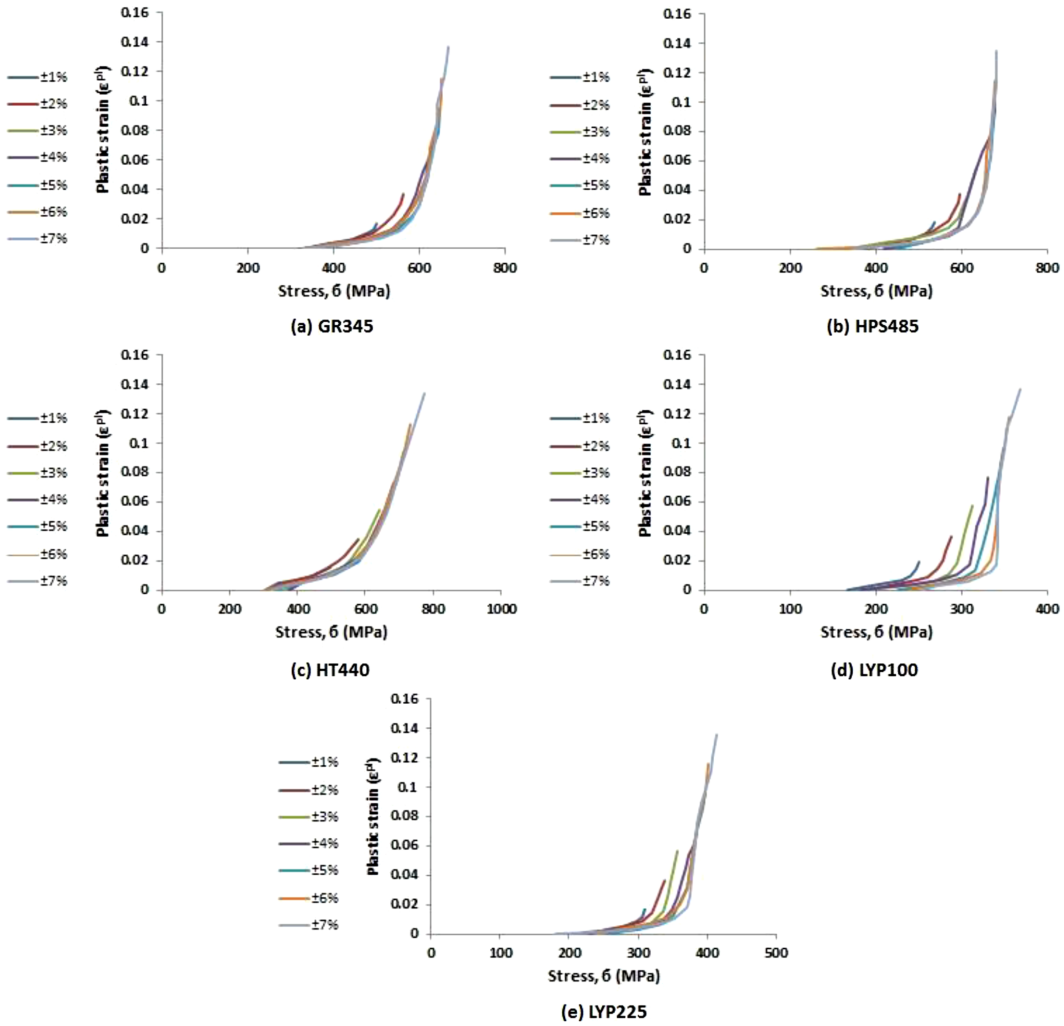

Figure 5. Kinematic characteristics.

Table 3. Kinematic parameters

Steel grade	Parameters	±1%	±2%	±3%	±4%	±5%	±6%	±7%
GR345	YIELD	415.46	450.24	481.16	479.23	496.62	490.82	500.93
	C1	14080	707.62	2089.7	1191.8	1019.9	958.99	746.26
	C2	0	11630	17896	17580	17353	15413	20362
	γ1	116.8	0	23.15	0	12.063	11.618	7.1362
	γ2	0	110.19	201.53	153.01	157.12	131.28	169.87
HPS485	YIELD	445.97	487.04	485.09	548.46	561.37	469.44	514.42
	C1	14648	5602.4	681.36	815.53	297.69	956.69	23850
	C2	0	5432.3	15408	13676	9623.9	40196	1179
	γ1	118.54	91.642	0	0	0	19.891	190.47
	γ2	0	93.897	116.46	149.24	95.223	236.51	25.909
HT440	YIELD	400.97	443.58	501.7	530.75	523	519.13	548.18
	C1	13019	6992.4	2662.4	664.29	1164.1	1293	1367
	C2	0	3229.7	5235.4	6508.2	11050	12783	11676
	γ1	3.867	51.649	44.59	0	0	0	0
	γ2	0	56.048	49.59	46.191	81.727	87.513	85.421
LYP100	YIELD	208.04	238.07	246.65	256.3	287.4	297.05	310.99
	C1	7869.6	333.95	407.18	322.63	311.18	181.47	224.15
	C2	0	6603.2	12458	11752	8082	6967.6	5976.7
	γ1	163.61	0	0	0	0	0	0
	γ2	0	147.32	232.43	186.57	174	147.93	156.93
LYP225	YIELD	276.74	283.99	298.49	303.32	327.49	322.66	296.94
	C1	804.04	422.29	349.79	593.01	437.08	345.32	366.14
	C2	3214.1	6811.9	8365.5	12141	8714.6	7175.6	21903
	γ1	0	0	0	0	0	0	0
	γ2	0	140.11	173.3	197.48	174.75	117.69	239.03

ε_1^{pl}). According to Eqs. (7) to (9) the kinematic hardening parameters, C_k and γ_k, can be calibrated for any material at any strain range. ABAQUS can do this calibration and reports the obtained parameter values through the data file. The number of back stresses defines the exactness of the kinematic component of the model, and in this paper, the number of back stresses is selected as "2", by which an appropriated accuracy is attained, thus, two sets of parameters are reported in the data file naming C_1, γ_1, C_2 and γ_2. The kinematic parameters obtained from the tabular data for any of the steel grades at any strain range between ±1 and ±7% ($\Delta\varepsilon$=2~14%) are summarized in Table 3. Comparing the yield points ($\sigma|_0$) presented in Tables 2 and 3, it is observed that these points are not the same for each material at any strain range, while the same values of yield strength should be introduced to ABAQUS for both of the isotropic and kinematic components. The yield stress achieved by the isotropic part should be introduced to the software for both of the components, because the isotropic component describes the yield surface according to the value of yield stress ($\sigma|_0$) (HKS, Hibbitt *et al*., 2012). However, in the case that only the kinematic part is utilized, the kinematic yield stress should be inserted to the software.

Similar to the case of isotropic hardening, the parameters should be selected for each analysis according to the strain range that the model experiences through that analysis. Also, in the case of loadings with stepwise increasing strain ranges (e.g. AISC (2005) or ATC-24 (1992)) the use of 'field variables' to define various series of parameters for any strain interval through the analysis may help to achieve a better accuracy.

On the other hand, in modeling of some materials, it may be better to use only one of the isotropic and kinematic hardening components instead of utilizing a combined model. Therefore, it is seen that proper validations are required in the utilization of the isotropic-hardening parameters.

2.3. Ramberg-Osgood model

As mentioned before, Ramberg-Osgood hardening models for these five steel grades were proposed in the previous study (Dusicka *et al*., 2007); however, in this research, for providing a better comparison of this model with isotropic-kinematic model, another form of the Ramberg-Osgood model is studied, as indicated in Eq. (10) (Ramberg & Osgood, 1943):

$$E\varepsilon = \sigma + \alpha\left(\frac{|\sigma|}{\sigma_0}\right)^{n-1}\sigma \tag{10}$$

Table 4. Ramberg-Osgood parameters

Steel grade	E	ν	σ_0	n	α
GR345	186200	0.3	353	7.338546	0.230676
HPS485	201300	0.3	503	8.201659	1.418534
HT440	208200	0.3	501	5.276879	0.649682
LYP100	153100	0.3	76.5	5.593868	0.019451
LYP225	195100	0.3	242	6.794433	1.426858

where α, σ^0 and n are the yield offset, the yield stress and the hardening exponent, respectively. The only virtue of this equation compared with "Power Equation" studied in the previous work (Dusicka *et al*., 2007) is that ABAQUS (HKS, Hibbitt *et al*., 2012) utilizes this formulation, hence, the required parameters of this formulation, including E, ν (Poisson's ratio), σ^0, n, and α, can be directly inserted to this finite element program, instead of specifying the formula or stress-strain points. According to the experimental results (Dusicka *et al*., 2007), the parameters n and α can be obtained from each material by the regression of the ultimate cyclic stress values through the strain ranges, as presented in Table 4. It should be noted that this model is suitable for monotonic loading in order to predict the skeleton curve (the backbone curve of the hysteresis diagram).

3. Validation of Hardening Material Hardening

In order to validate the obtained parameters, and also to show how they can be utilized in the simulation of structural components, in this section, four experiments conducted by Dusicka *et al*. (2010) are simulated in ABAQUS and the results are compared with those of the experimental results as well as those of the Ramberg-Osgood model (1943).

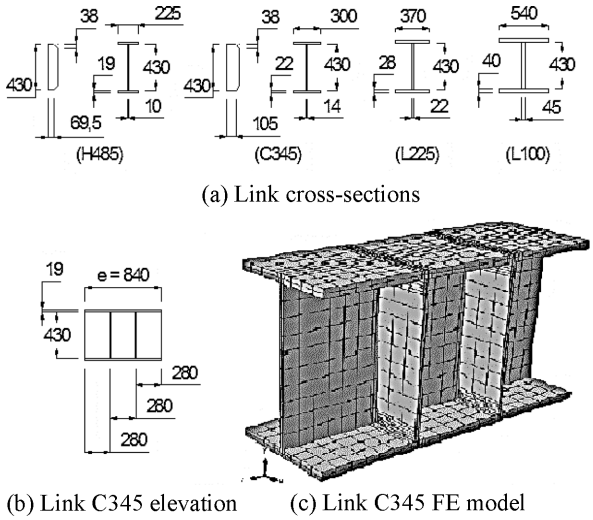

(a) Link cross-sections

(b) Link C345 elevation (c) Link C345 FE model

Figure 6. Details of the Links.

3.1. Model definition

For the purpose of simulation, finite element program ABAQUS-V6.12.1 (HKS, Hibbitt *et al*., 2012), which has a high ability of nonlinear analysis, was used in this study. Each of the four selected shear links were constructed of one of the steel grades LYP100, LYP225, A709 Conventional Grade (GR.345) and High Performance Steel (HPS485), naming L100, L225, C345 and H485, respectively, and

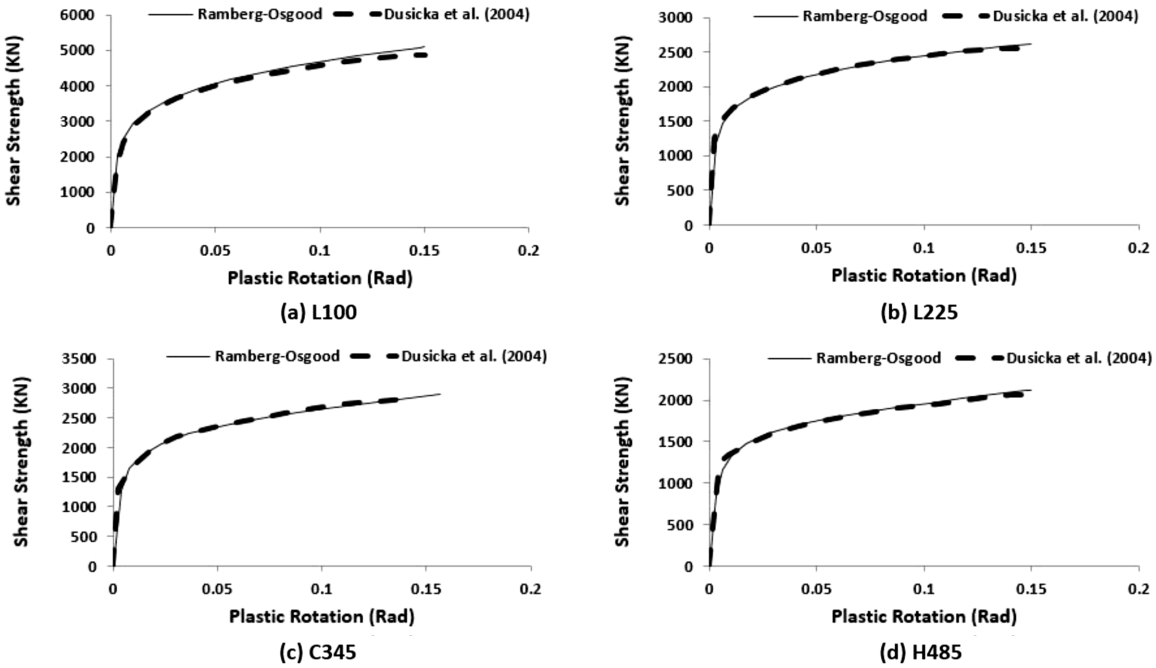

Figure 7. Comparison of the Ramberg-Osgood results.

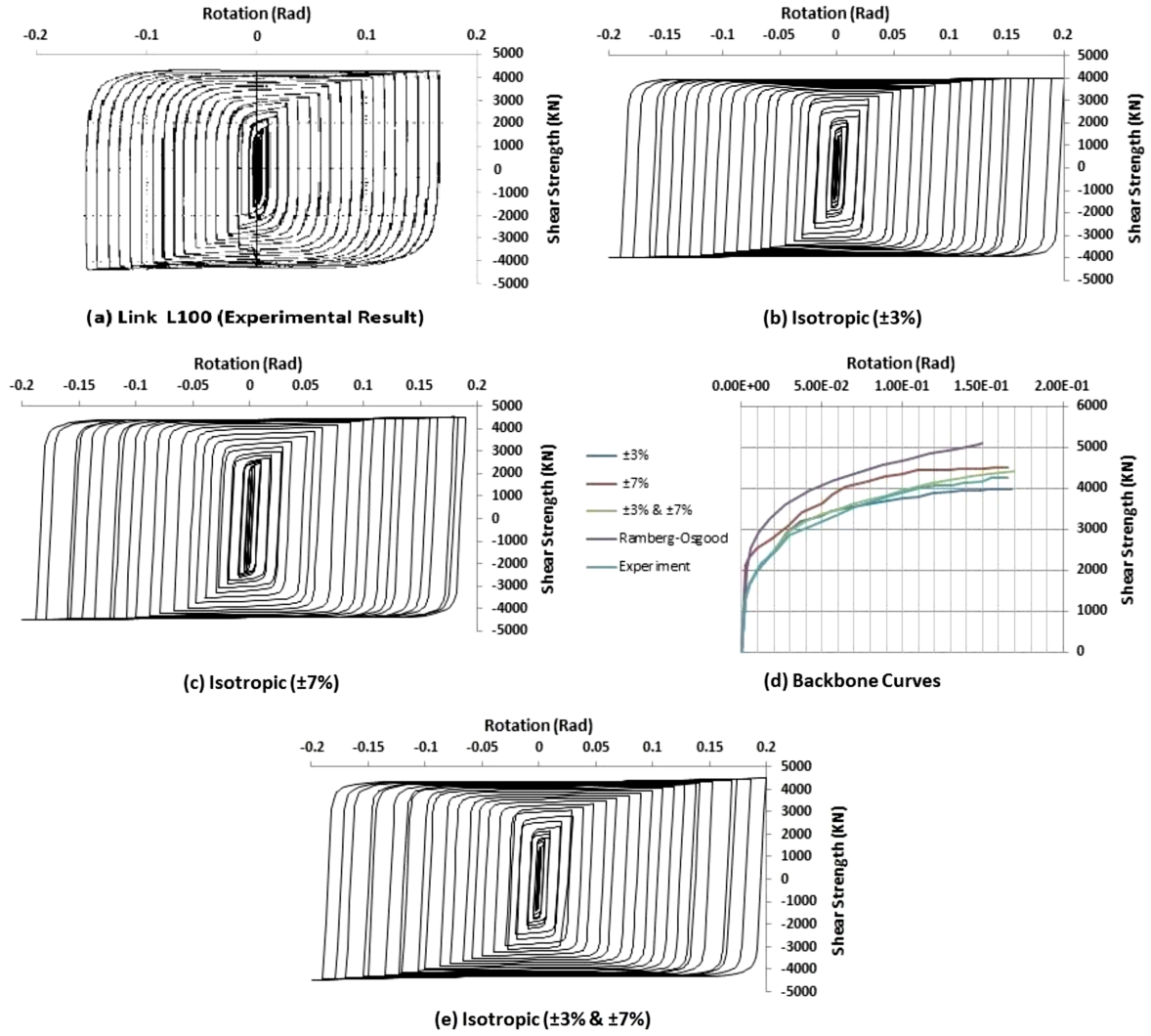

Figure 8. Comparison of stress-strain predictions of the Link L100.

designed such that all of them have almost the same values of plastic shear (V_p) and plastic moment (M_p). Therefore, it is obvious that their cross-sections varied as the material grades were not the same, as shown in Fig. 6(a). In the analytical simulations carried out by Dusicka *et al*. (2004) in which a material model identical to Ramberg-Osgood model were examined, the link models, including the two end connection zones and the effective part (the portion of each link including its effective length (e =840 mm)) for each link, were subjected to a monotonic effective rotation (γ_{eff}) applied to one end of the connection zones in vertical direction, while the other degrees of freedom, exempt the longitudinal transverse direction, were restrained. The other connection zones were fixed against displacement in any direction. Those boundary conditions were identically duplicated in the current project, however, for simplicity's sake, only the effective parts of the links were modeled and cyclic semi-static strain-controlled load (γ_p), according to AISC seismic provisions (AISC, 2005), was applied directly to the effective parts of the shear links (instead of applying γ_{eff} to the connection zones). For clarification, the longitudinal view of the link C345 with its two stiffeners is depicted in Fig. 6(b).

Also, in the finite element models proposed in 2004 (Dusicka *et al*., 2004), in order to provide a better investigation of stress and plastic strain concentrations through the thickness of the models as well as accurate weak axis bending, five layers of the solid 8-node continuum element with reduced integral, named as C3D8R in ABAQUS (AISC, 2005), were assigned to the flanges and stiffeners, where mesh refinements for the regions anticipated to undergo excessive plastic deformations were accommodated; however, in the current study, although appropriate mesh refinements were provided for the stiffener to web and flange connection regions, two layers of mesh were chosen for the thickness of flanges, webs and stiffeners, as shown for the link C345 in Fig. 6(c). Also, as it has been found that these models are not vulnerable to imperfections, it was concluded that the

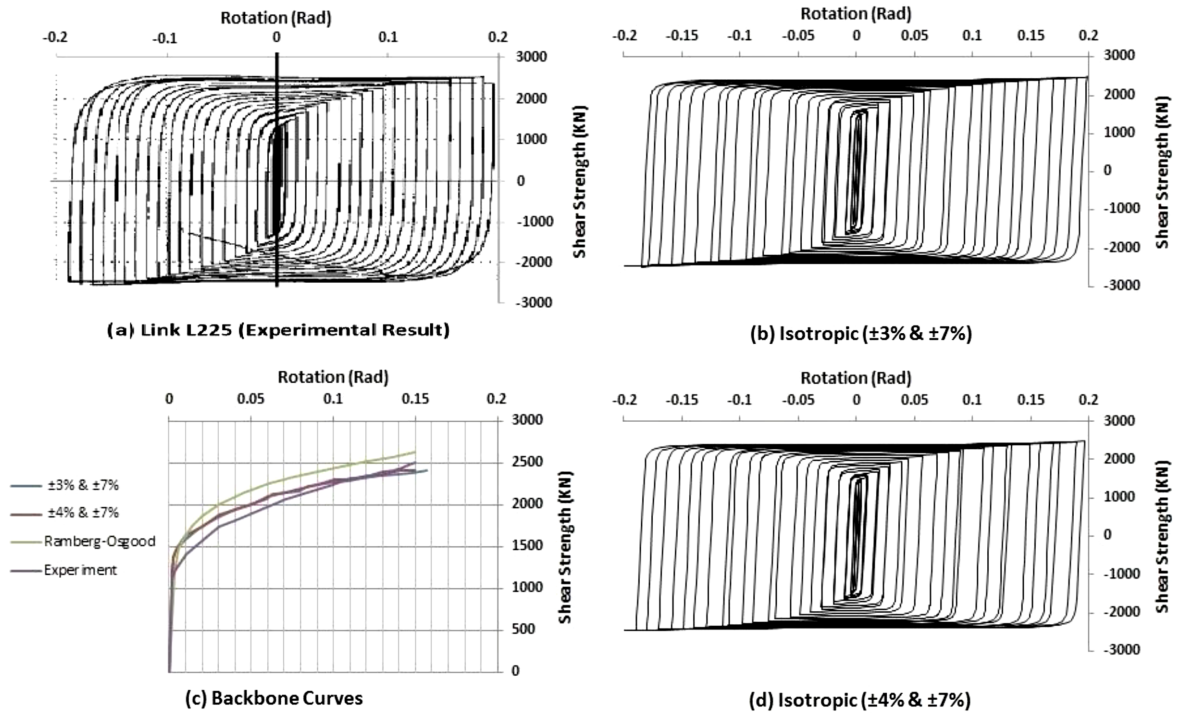

Figure 9. Comparison of stress-strain predictions of the Link L225.

absence of initial imperfection through the analysis does not matter to the accuracy of the results.

Before validating the isotropic-kinematic hardening material model, it is required to verify the accuracy of the finite element models. For this purpose, the finite element models proposed in 2004 (Dusicka *et al*., 2004) are examined by the Ramberg-Osgood material parameters found in the previous section, as summarized in Fig. 7. Some marginal differences are observed between the results that are mainly because of the differences in material modeling methods. Dusicka *et al*. (2004) utilized the peak cyclic stress values at each strain range, while the Ramberg-Osgood material model utilizes the regression of these peak stress-strain points. Ignoring these small differences, it is observed that although the current model is very simplified, it has an acceptable accuracy, providing the opportunity to proceed to the validation of the isotropic-kinematic parameters.

3.2. LYP100 material

Figure 8(a). shows the cyclic stress-strain response of the link L100 (constructed of LYP100 material) obtained from the experiment (Dusicka, *et al*., 2010). It is observed that the size of yield surface (the yield strength of the stress-strain diagram) is increased after each cycle, therefore, it is concluded that the cyclic hardening behavior of this material can be simply simulated by using only its isotropic component parameters, $\sigma|_0$, Q_∞, and b. But the main problem is the matter of choosing these parameters from an appropriate strain range ($\Delta\varepsilon$) which reflects the strain range experienced in the analysis. In the first step, the parameters corresponding to the strain ranges ±3 and ±7% (Table 2) were examined and the results are summarized in Fig. 8(b) and 8(c), while their backbone curves are compared in Fig. 8(d). It is observed that the material parameters obtained from the strain range ±3% can predict accurately the initiation of nonlinearity and remain appropriate till the rotation of about 0.03 (Rad), but cannot predict the ultimate stress-strain behavior of the link, in contrast to those corresponding to the strain range ±7% that only gives a proper prediction of the ultimate hardening. Thus, as it was indicated earlier, in order to achieve a more accurate result, the utilization of 'field variables' may be very helpful. Accordingly, in the second step, utilizing field variable technique, a model with the ±3% strain parameters till the rotation of 0.03 (Rad), and after that with the parameters of ±7% strain range was utilized, and its hysteresis response is shown in Fig. 8(e) with its backbone curve compared with the other results in Fig. 8(d). It can be observed that a relatively exact model is obtained by utilizing both series of parameters (±3 and ±7%) together, especially in comparison to the Ramberg-Osgood material model (Fig. 8(d)).

3.3. LYP225 material

The hysteresis curve of the link L225 obtained from the experiment (Dusicka *et al*., 2010) is depicted in Fig. 9(a). similar to the link L100, this link is expected to have a fully isotropic hardening behavior. Hence, a combination of isotropic hardening parameters, for the strain ranges ±3 and ±7% (Table 2) is considered as the first try, and the resulted hysteresis and backbone curve are shown in

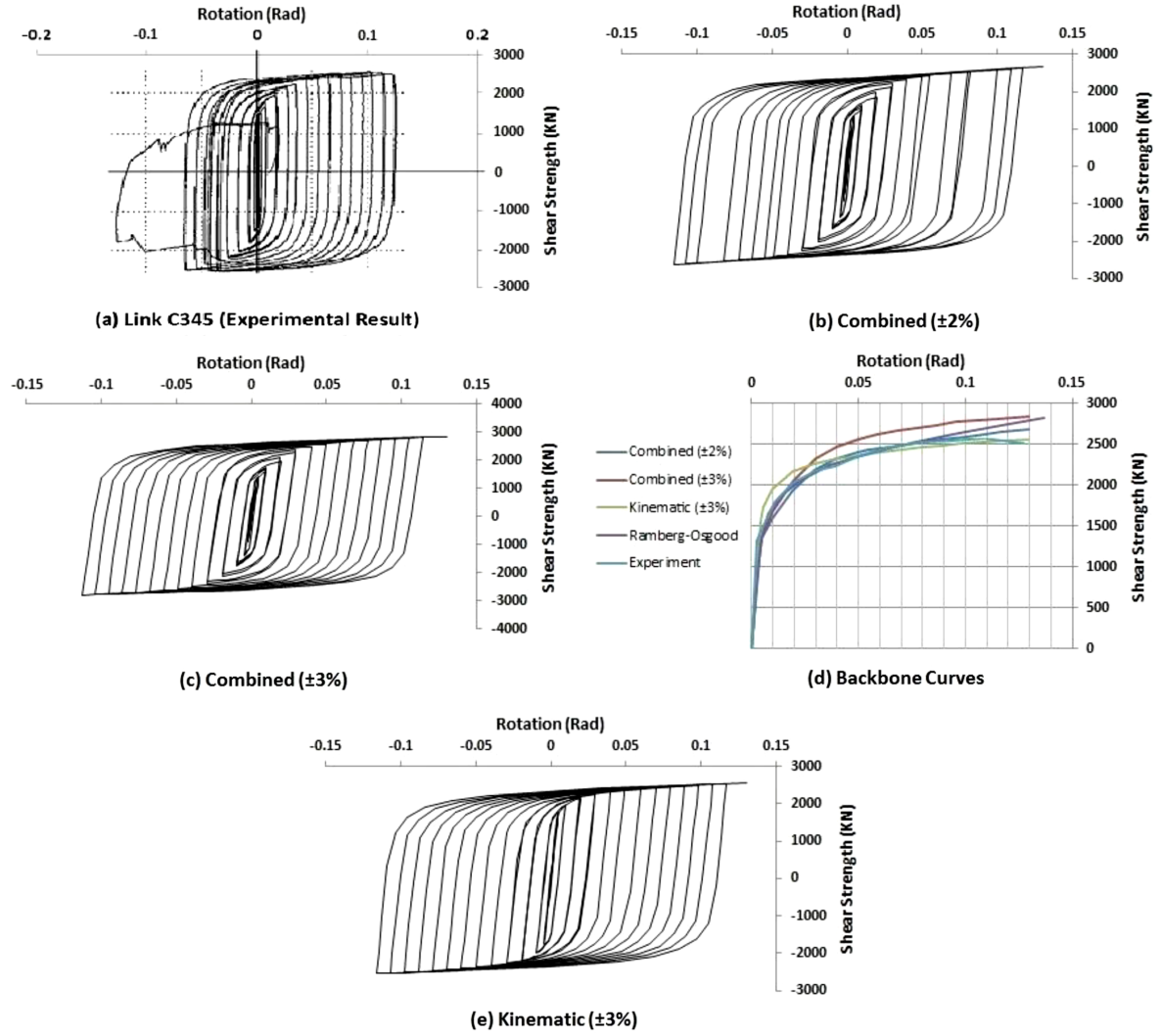

Figure 10. Comparison of stress-strain predictions of the Link C345.

Figures 9-b and c. However, this model cannot predict the hardening behavior of the last cycles. It is justified by noticing that the link L225 experienced extreme plastic rotation as well as a heavy web buckling (Dusicka *et al*., 2010) that may have been lead to undergoing strain values larger than ±7%. But, the combination of isotropic parameters of the strain ranges ±4 and ±7% has shown a slightly better estimation and its hysteresis and back bone curves remained accurate till more than the plastic rotation value of 0.14, as shown in Fig. 9(c) and 9(d), which is satisfactory for most of the engineering analyses.

3.4. GR345 material

Figure 10(a) (Dusicka *et al*., 2010) demonstrates the experimental stress-strain diagram of the link C345, made out of GR345 steel grade. It can be seen that hardening behavior of this steel grade in early cycles is isotropic as the size of the yield surface increases, and after some cycles, the behavior proved kinematic as only the transition of the yield surface is observed after each cycle (no leap occurs in the yield strength). Therefore, in the first step, the combination of isotropic and kinematic hardening component parameters extracted from the strain range ±2% is examined as well as that of the strain range ±3% (Tables 2 & 3), as shown in Fig. 10(b) and 10(c). Comparing the backbone curves, as shown in Fig. 10(d,) it can be seen that the material data corresponding to the strain range ±2% gives a better estimation of the cyclic hardening behavior as compared to that of ±3%. Comparing these results with that obtained from Ramberg-Osgood model, as shown in Fig. 10(e), it is seen that although Ramberg-Osgood model is very exact in predicting the stress-strain behavior of this material in early cycles, the total behavior is better estimated by the combined isotropic-kinematic model (with the strain range of ±2%).

As another try, this material is modeled by only the kinematic component parameters of the strain range ±3%, and the hysteresis result is shown in Fig. 10(e). Compared with the backbone curve of other cases in Fig. 10(d), although this model is relatively inaccurate in estimating

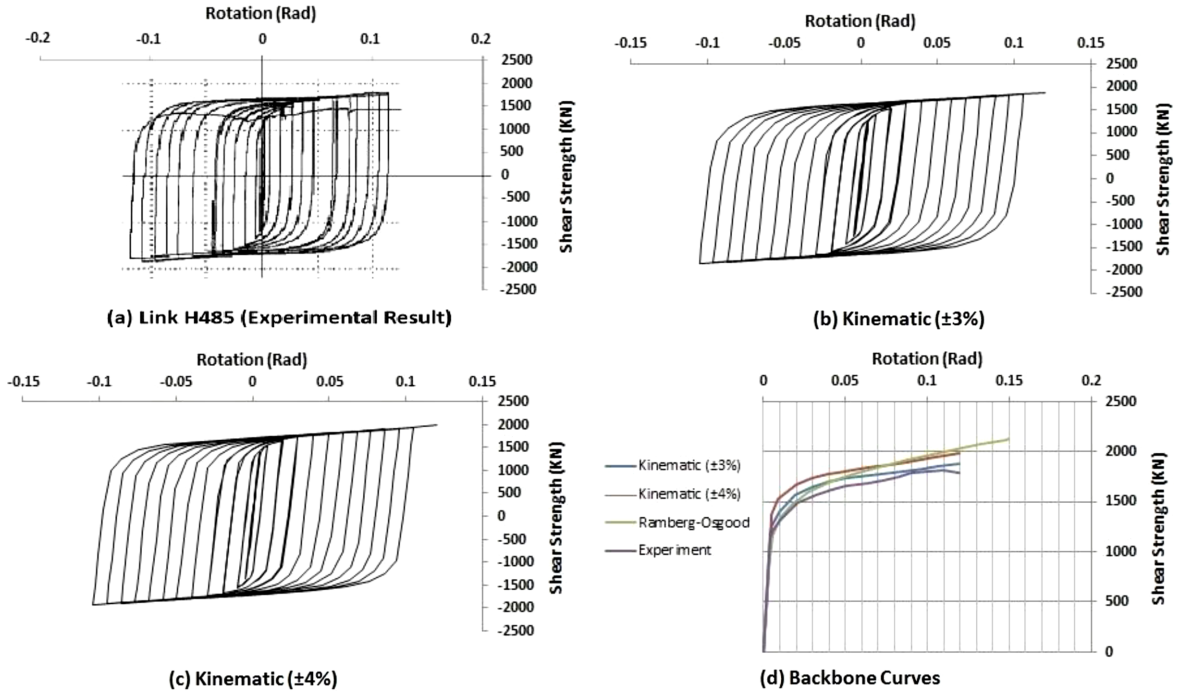

Figure 11. Comparison of stress-strain predictions of the Link H485.

the stress-strain behavior of the material in primary cycles, it can predict adequately the ultimate behavior of the material.

3.5. HPS485 material

According to the hysteresis diagram of the link H485 (Dusicka *et al*., 2010), as presented in Fig. 11(a), it can be found that HPS485 steel has kinematic hardening behavior as no leap is observed in the yield strength (the size of yield surface) through the cycles. Thus, it is anticipated that the cyclic hardening of this material can be modeled by specifying only the kinematic hardening component. Hence, the link is modeled by the kinematic parameters of the strain ranges ±3 and ±4% (Table 3), and the obtained hysteresis curves are summarized in Fig. 11(b) and 11(c). A comparison of the backbone curves, as shown in Fig. 11(d), indicates that the kinematic material parameters corresponding to the strain range ±3% give a more appropriate estimation of cyclic stress-strain behavior of this material, compared with the ±4% parameters and the Ramberg-Osgood model.

I should be noted that although it is required to conduct more experimental and analytical studies to judge about the optimum series of parameters for achieving an accurate cyclic hardening model for H440 steel grade, according to the fact that roughly no isotropic hardening was observed for this material, as shown in Fig. 2(c), it is anticipated that H440 can be modeled by specifying only the kinematic hardening component. Even for the four validated steel grades, the issue of choosing the appropriate strain range(s) is excessively dependent on the shape of the structural member and the loading protocol that may vary from one case to another; however, this problem can be easily solved by few tries when validating the finite element model for any specific case.

4. Conclusion

The isotropic-kinematic cyclic hardening of five steel grades was studied in this research and the calibrated isotropic and kinematic hardening parameters were proposed. Afterwards, four of these steel types were validated by simulating four experimented shear links in the finite element program ABAQUS and the results are summarized as the following:

(1) Combined isotropic-kinematic hardening model, which divides the cyclic hardening characteristic of metals into two separate components, including isotropic and kinematic, is proved more exact in simulating the cyclic stress-strain behavior of various steel grades in comparison to Ramberg-Osgood model;

(2) Low yield point steel grades can be accurately modeled by utilizing only the isotropic hardening component parameters $\sigma|_0$, Q_∞, and b);

(3) A709 conventional grade 345 steel model shows the best accuracy while introducing both of isotropic and kinematic hardening components, while the utilization of only the kinematic hardening component can result in an appropriate estimate;

(4) A709 high performance steel grade 485 can be modeled appropriately by introducing only the kinematic hardening component;

(5) For HB-HT440 steel grade, it is highly anticipated that this grade can be simply modeled by introducing only the kinematic hardening component, although for a more definite judgment experimental validation is required.

References

AISC, A. I. S. C. (2005). *Seismic Provisions for Structural Steel Buildings.* Chicago, IL: American Institute of Steel Construction, AISC/ANSI 341-10., California, U.S.

ATC, A. T. C. (1992). *Guidelines for cyclic seismic testing of components of steel structures.* RDD Consultants, Inc., Redwood City, California, U.S.

Chaboche, J. L. (1989). "Constitutive equations for cyclic plasticity and cyclic visco-plasticity." *International Journal of Plasticity,* Volume 5, pp. 247-302.

Dusicka, P. and Itani, A. M. and Buckle, I. G. (2004). "Finite element investigation of steel built-up shear links subjected to inelastic deformations." *Earthquake Engineering and Engineering Vibration,* 3(2), pp. 195-203.

Dusicka, P. and Itani, A. M. and Buckle, I. G (2007). "Cyclic response of plate steels under large inelastic strains." *Journal of Constructional Steel Research,* Volume 63, pp. 156-164.

Dusicka, P. and Itani, A. M. and Buckle, I. G. (2010). "Cyclic Behavior of Shear Links of Various Grades of Plate Steel." *Journal Of Structural Engineering,* 136(4), pp. 370-378.

HKS, Hibbitt, D. and Karlsson, B. and Sorensen, P. (2012). *ABAQUS standard user manual Version 6.12.1.* s.l.:Inc., Pawtucket, RI.

Kuþyýlmaz, A. and Topkaya, C. (2013). "Design overstrength of steel eccentrically braced frames." *International Journal of Steel Structures,* Volume 13, pp. 529-545.

Lemaitre J, Chaboche J.L. (1990). *Mechanics of Solid Materials.* Cambridge University Press, Cambridge, U.K.

Ramberg, W. and Osgood, W. R. (1943). "Description of stress-strain curves by three parameters." Technical note no. 902. National Advisory Committee on Aeronautics.

Shi, G. and Wang, M. and Bai, Y. and Wang, F. and Shi, Y. and Wang, Y. (2012). "Experimental and modeling study of high-strength structural steel under cyclic loading." *Engineering Structures,* Volume 37, pp. 1-13.

Shi, Y. and Wang, M. and Wang, Y. (2011). "Experimental and constitutive model study of structural steel under cyclic loading." *Journal of Constructional Steel Research,* Volume 67, pp. 1185-1197.

Wang, Y. B. and Li, G. Q. and Cui, W. and Chen, S. W. and Sun, F. F. (2015). "Experimental investigation and modeling of cyclic behavior of high strength steel." *Journal of Constructional Steel Research,* Volume 104, pp. 37-48.